stellarator news

Published by Fusion Energy Division, Oak Ridge National Laboratory
Building 9201-2 P.O. Box 2009 Oak Ridge, TN 37831-8071, USA
Editor: James A. Rome Issue 34 July 1994
E-Mail: jar@ornl.gov Phone: (615) 574-1306

The ATF Finale

Emphasizing long-pulse operation, the Advanced Toroidal Facility (ATF) experiment has concluded its final experimental stage before being mothballed. (See the article by T. C. Jernigan in the May issue.) The ATF experiment has achieved pulse lengths up to 1 hour. Figure 1 shows the evolution of the discharge of the longest pulse length (3693 s). The helium discharge was heated by a 28-GHz gyrotron with P_{ECH} = 70 kW at B = 0.54 T. Gas feedback control was used to maintain a constant electron density ($\overline{n}_e = 3 \times 10^{18}$ m^{-3}). The discharge was terminated by a ground fault in the helical field system. Keying the gas feedback control to the vessel pressure (rather than the plasma density) has led to better plasma performance than that with the constant density feedback shown here. However, the longest pressure feedback discharge was limited to 1576 s.

Long-pulse operation was very effective in wall conditioning, reducing residual gases (i.e., Mass 18 and 28) in the RGA analysis to the lowest levels observed in the history of ATF, despite the fact that only a few days had passed since a vacuum opening. Long-pulse operation with hydrogen (rather than helium) did not last long because a few long-pulse shots loaded the vessel wall with hydrogen. More analysis is being carried out and will be published in the next issue of Stellarator News.

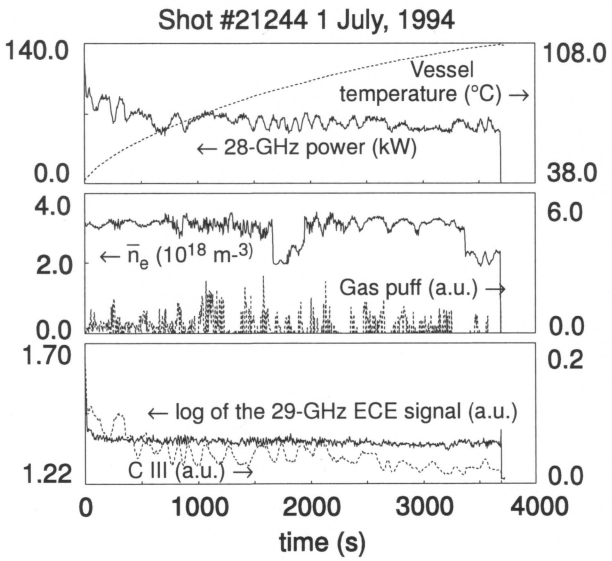

Fig. 1. Parameters for the longest discharge achieved in ATF

Masanori Murakami for the ATF Team
Oak Ridge National Laboratory
P.O. Box 2009, Bldg. 9201-2, MS 8072
Oak Ridge, TN 37831-8072 USA

Phone: (615) 574-1175
E-Mail: murakami@fed.ornl.gov

In this issue . . .

Around the Labs

Magnetic flux mapping on the Uragan-2M torsatron

Magnetic flux mapping studies have been performed for a torsatron with an additional toroidal field, Uragan-2M. Previous experiments with the "stellarator diode" technique have shown [1] that there is a rather sharp border for the volume with the strong probe current suppression and that the shape of this border corresponds to the shape of the last closed magnetic surface obtained from magnetic surface calculations.

In a new experiment "the luminescent rod" technique has been applied for magnetic surface tracing at reduced dc magnetic field value (0.1 T). The images of the spots produced by the impact of an electron beam against the luminescent rod were taken by a photocamera and processed by computer. The magnetic surfaces were measured at the toroidal plane [j = 0É for different values of parameter of $K_\varphi = I_{th}/(I_{th} + I_{tt})$]; I_{th} and I_{tt} are the toroidal fields produced by helical and toroidal coils, respectively.

In general, the results of measurements are in good agreement with calculations. However, a systematic difference was observed between calculated and measured rotational transform profiles for all K_j values: calculated profiles are observed in the experiment for larger (by 5 to 10%) values of K_j. This discrepancy can be explained by the fact that in our previous calculations each pole of helical winding was modeled by a relatively small number of current filaments.

In the range of K_j values of 0.33 to 0.36, closed, nested surfaces are observed (Fig. 1). When $K_j > 0.36$, the rational value of i = 1/2 occurs in the plasma, and 1/2 islands are observed. The islands' size and position are similar to those observed in our previous calculations [2], modeling magnetic field perturbations produced by the helical winding current feeds. Similarly, when K_j = 0.33, i = 1/3 occurs, and small (dr = 1–2 cm) 1/3 islands are observed.

The regime with $K_j = 0.34$ was chosen as a starting point for experiments on ion cyclotron resonant (ICR) plasma production and heating. A slow-wave antenna, shaped to match the plasma border, was installed in the vacuum chamber near the calculated last closed magnetic surface with an average radius of 21 cm. It appears that the antenna is inside of the last closed magnetic surface, so a movable limiter could be used to detach the antenna from plasma.

Yu. Kuznetsov for U-2M group
Institute of Plasma Physics
Kharkov , Ukraine
E-Mail: yuk@ipp.kharkov.ua

References.

[1] O. S. Pavlichenko, Plasma Physics and Controlled Fusion, **12**, Suppl.(12)B (1993) B223 .

[2]. N. T. Besedin, G.G.Lesnjakov, I.M.Pankratov, VANT, Ser. Controlled Fusion, No. 1 (1991) 48 (in Russian).

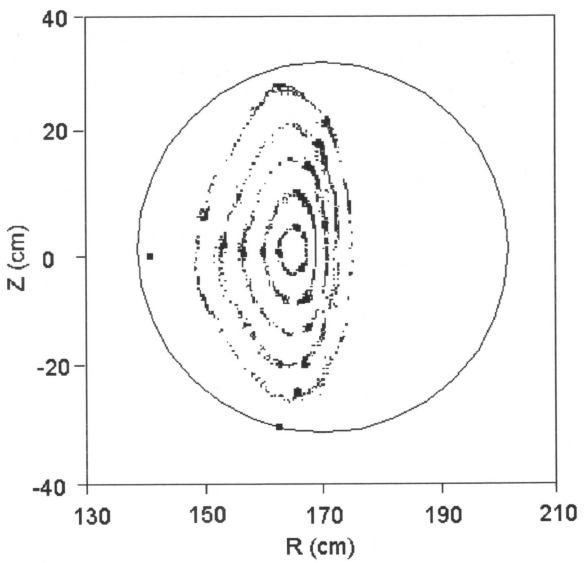

Fig. 1. Measured flux surfaces in U2-M with i between 0.33 and 0.36.

Detection of the Free Boundary Plasma Shift on Heliotron-E

Magnetic measurements are invariably an important part of plasma diagnostics in tokamaks and stellarators. In particular, knowledge and control of the plasma column shift is essential for sustaining high-beta toroidal plasmas. The magnetic measurement techniques developed for tokamaks can also be applied to stellarators. Essentially one must measure the poloidal magnetic fields related to the plasma Pfirsch-Schlüter current in a stellarator. In this article we present the external magnetic diagnostics that were used to determine the free boundary plasma shift of the plasmas in the Heliotron-E high-beta experiment during the period June 1993 – March 1994. We have studied the change of the free-boundary plasma shift as a function of the initial plasma position and the rotational transform.

The experiment was performed at 0.62 T, 0.94 T, 1.26 T and 1.9 T to match the electron cyclotron resonance heating (ECRH) power available at 53 and 35 GHz. Neutral beam injection (NBI) of up to 3.5 MW provides additional heating of the ECRH plasma. The injection angles of neutral beams are 0° ,11°, and 28° from the direction perpendicular to the torus. We have also performed experiments using coinjection (the direction of neutral beam is the same as that of equivalent current of the helical field).

The principle behind determining the free-boundary plasma shift in a stellarator is to interpret the change of the poloidal magnetic field due to the plasma-induced dipole (Pfirsch-Schlüter) current. We have used one pair of poloidal magnetic flux loops that are set in the equatorial plane. One pair of cosine coils is separated by a half helical period. A theory to analyze the normalized free-boundary plasma shift is given by Pustovitov [1]. We have also measured the stored energy with a diamagnetic loop.

Figure 1(a) shows the resulting free-boundary plasma shift $\Delta b/\ a_p \leq 1.3$ ö 10^{-2}, where a_p is the average plasma radius. In this discharge, the hydrogen plasma is produced at 0.61 T by a 35-GHz microwave power source (from ORNL) and heated some more by NBI (0.65 MW at 28° and then 3.2 MW at 0°, 11°, 28°). The diamagnetic measurement shows that the volume-averaged beta value is 0.95%, and the stored energy is 5 kJ as shown in Figs. 1(b) and (c). Figures 1(a) and (b) show good proportionality between the measured free-boundary plasma shift and the volume-averaged diamagnetic beta. The toroidal current I_p (â 2kA) flows first to the same direction as beam and then reverses. The total radiative power loss (700 kW) is measured with a bolometer. The line-averaged density increases linearly with time from 1.0 ö 10^{13} cm^{-3} to 6.0 ö 10^{13} cm^{-3} . The central temperatures are in the range 200 to 230 eV at 400 ms.

The free-boundary plasma shift was measured for a confining helical magnetic field of 0.62 T, 0.94 T, 1.26 T. and 1.9 T for the standard magnetic configuration in Heliotron-E [with R = 2.2 m, a_p = 0.21 m, vacuum rotational transforms ɨ(0) ~ 0.53 and ɨ(a_p) ~ 2.8]. We find that the proportionality between the plasma shift and the volume-averaged beta is nearly 1.8... bÓ$_{dia}$ for the standard configuration. We compared the experimental observation of the shift ($\Delta b/\ a_p$ versus ... bÓ$_{dia}$) with the theoretical calculation of the plasma boundary shift [1]. The measured shift is in the range between the expected upper limit ($\Delta b/\ a_p$ = b(0)/2b$_{eq}$) and the lower limit ($\Delta b/\ a_p$ = ... bÓ/2b$_{eq}$), where b$_{eq}$ = [ɬ (a_p)]^2 (a_p/ R_p) ~ 0.77 for the standard Heliotron-E configuration.

The measured free-boundary plasma shift strongly depends on the initial plasma position (R) and the rotational transform. We have studied the free-boundary shift($\Delta b/\ a_p$) by changing the initial position of the plasma column (R = 2.21 m – 2.14 m) by changing the auxiliary vertical field coil current from shot to shot. This configuration scan also changes the vacuum rotational transform at boundary [ɨ(a_p) = 2.4 – 3.2)]. Plasma was produced at a magnetic field of 0.94 T by ECRH with three 53-GHz microwave sources and then heated by 3.0 MW of NBI.

Figure 2(a) shows the free-boundary plasma shift and the average beta in the outward-shifted configuration. These data show that for the outward-shifted case the free-boundary shift [Fig. 2(a)] is larger (30%) than that of the standard configuration [Fig.2(b)] at the same average beta. The absolute value of average plasma boundary shift is within 3 mm.

Figure 2(e) shows the measured free-boundary plasma shift and the average beta in the inward-shifted vacuum magnetic configuration with parameters R = 2.14 m, DR = -6 cm, ɨ(a_p) = 2.4, ɨ(0) = 0.51, b* Ü B_v/B_{hf}(0)= -0.206. These data show that the magnetically measured free-boundary plasma shift decreased remarkably in the inward-shifted configuration. In fact, the plasma-induced vertical field, which was monitored by the psi-loops, also decreased. This result suggests that the inward-shifted configuration would be a configuration with reduced Pfirsch-Schlüter current in the Heliotron-E device.

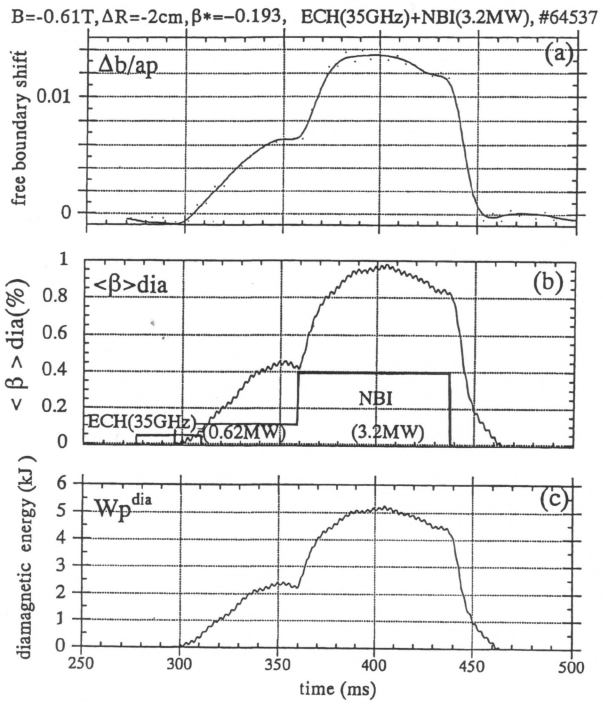

Fig. 1. (a) Time evolution of the free-boundary plasma shift, (b) diamagnetic average beta, (c) diamagnetic stored energy. The hydrogen plasma is produced at 0.61 T by a 35-GHz microwave power source, and further heating is supplied by NBI (0.65 MW at 28° and then 3.2 MW at 0°, 11°, 28°). The magnetic configuration is the inward-shifted case (DR = -2 cm) with the additional vertical field
b* =$B_v/B_{hf}(0)$ = - 0.193. A weak additional toroidal field is also superposed [a*=$B_t/B_{hf}(0)$ = +0.05] to improve the plasma production and confinement in this discharge.

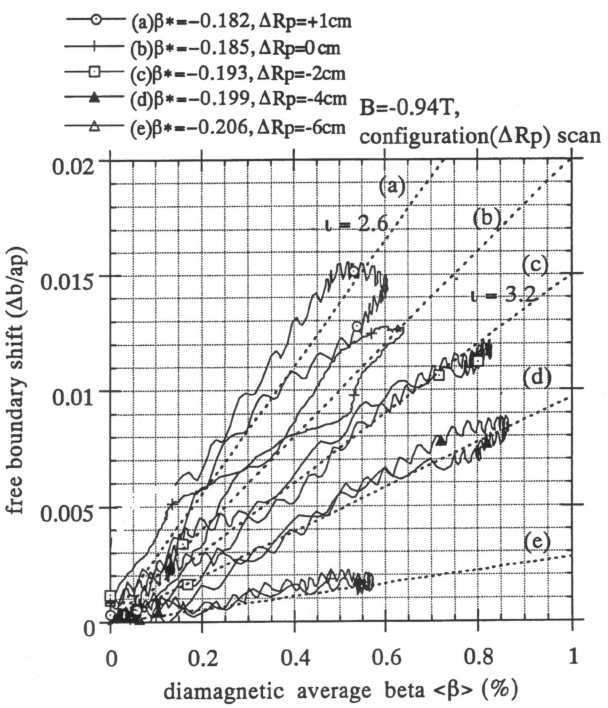

Fig. 2. Dependence of the free boundary plasma shift on the initial plasma position (R) and the rotational transform. The magnetic field is 0.94T. (a) the outward-shifted configuration with the vacuum rotational transform given by $\iota(a_p)$ = 2.6 and $\iota(0)$ = 0.57; (b) the standard configuration with $\iota(a_p)$ = 2.8 and $\iota(0)$ = 0.53; (c) the inward-shifted config. with $\iota(a_p)$ = 3.2 and $\iota(0)$ = 0.47; (d) the inward-shifted config. with $\iota(a_p)$ = 2.9 and $\iota(0)$ = 0.47 (e) the inward-shifted config. with $\iota(a_p)$ = 2.4. and $\iota(0)$ = 0.51.

The optimum beta and the energy content are also obtained in the inward-shifted position [R = 2.16 m, $\iota(a_p)$ = 3.2, $\iota(0)$ = 0.47] as shown in Fig. 2(d). The heating NBI power (3 MW) and the line-average density (5 to 6 ö 10^{13} cm^{-3}) are nearly constant in the configuration scan.

In summary, we have applied poloidal magnetic diagnostics to determine the free-boundary plasma shift in a stellarator/heliotron plasma. The typical measured plasma boundary shift $\Delta b/\ a_p$ in the standard Heliotron-E configuration is 8 to 12 ö 10^{-3},when the volume-averaged beta is 0.50%. Measured normalized plasma boundary shift is nearly proportional to the diamagnetic volume-averaged beta, which can go up to 0.95%. The magnetically determined plasma boundary shift Db is < 3 mm.

We find that the measured plasma boundary shift strongly depends on the initial vacuum magnetic configuration parameters, such as the horizontal position of magnetic axis and the rotational transform. When the vacuum magnetic axis is shifted inward toward the major axis, we observed a significant decrease of the normalized plasma shift ($\Delta b/\ a_p$) and the plasma-induced vertical field, possibly due to a reduction of the Pfirsch-Schlüter current.

More information from these studies will be presented at the EPS conference (June 27, Montpellier, France).

Sakae Besshou for the Heliotron E group
Plasma Physics Laboratory
Kyoto University
Gokasho Uji, Kyoto , Japan

Phone: (81) -774-32-3111 ext.3432
Fax: (81) -774-33-0865
E-mail: besshou@ppl.kyoto-u.ac.jp

Reference

Improvement of ICRF heating after boronization in CHS

Ion cyclotron radio frequency (ICRF) heating experiments (H minority heating: 26 MHz, $B_t \sim 1.7$ T, $P_{rf} <$ 1 MW) have been carried out since October 1993 and are scheduled to continue until the end of this year. However, progress was usually limited by increasing impurities. It was very clear that the impurity sources were the ICRF antennas (4 P-ports + 1 U-port) toroidally arranged to maintain a 1.5-cm clearance to the LCFS at $R_{ax} = 92.1$ cm. The most important thing is to reduce radiation loss from oxygen, which radiates strongly in the edge region only. Therefore, boronization was restarted to achieve impurity control during the ICRF experiment.

Boronization was carried out twice using decaborane, and a total of 10 g of decaborane was introduced into CHS; 5 g of boronization makes a boronized surface with an average thickness of 800 Å in each case. The boronization was very effective for our ICRF experiment, whereas it has not shown a clear advantage for NBI heating with titanium (Ti) gettering except for a small increase in the stored energy (W_p) in a high-density region [1]. After boronization, the metal impurity (titanium) completely disappeared, and oxygen radiation was largely reduced. The reason originates in the difference in accessibility for ICRF antennas between the Ti-gettering and the boronization. The flashing area of the Ti-gettering in CHS covers 70% of the total vacuum surface. This covering, however, is largely reduced for the ICRF antennas because of their complex geometrical features. In contrast to this, the boronization is very effective for covering the antennas, since it is carried out using He-glow discharge.

Figure 1 shows plasma stored energies obtained for both cases of Ti-gettering and boronization. The input power of the ICRF pulse was 700 kW for both cases. The density was limited below 3 ö 10^{13} cm^{-3} in the case of Ti-gettering, and the W_p did not show any increase for the increased density. Nevertheless, the density limit extended up to 5 ö 10^{13} cm^{-3} for the boronization case. The W_p increased up to 60% of the LHD scaling level. Here, it should be noticed that an injected power of 700 kW was used as an input power in the scaling calculation.

A typical time trace of the experiment is shown in Fig. 2. During the ICRF pulse with a density rise up to 5 ö 10^{13} cm^{-3} the radiation power was kept to a constant level of 170 kW. This was a main reason why the electron density could be raised up to 5ö10^{13} cm^{-3}. The electron density and temperature profiles are measured for these experiments, as shown in Fig. 3. The comparison is also made between the Ti-gettering and boronization cases. The electron density was adjusted to 3 ö 10^{13} cm^{-3} at the central column of the plasma for both cases. The RF power injected was 300 kW and 700 kW for the Ti-gettering and boronization cases, respectively. In the case of the Ti-gettering the plasmas were not reproducible for higher injection power because of the radiation collapse.

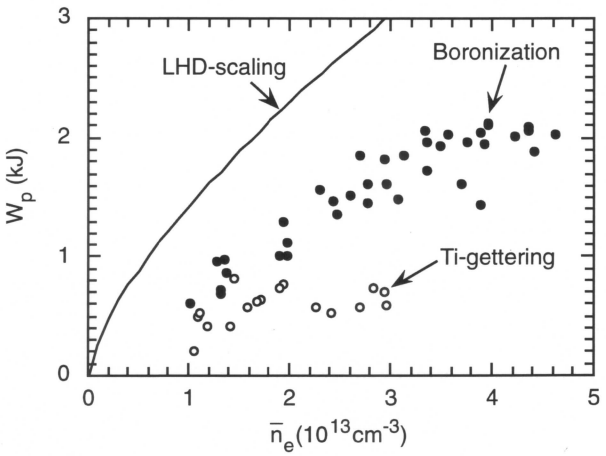

Fig.1. Comparison of plasma stored energy W_p between Ti-gettering and boronization cases. The RF power is 700kW. The solid line shows LHD scaling.

The electron density profiles obtained are roughly the same, and they indicate flat or hollow features. It seems that the tendency toward a hollow profile is enhanced for the boronization case, although the plasma is not steady state. Normally, for this configuration (R_{ax} = 92.1 cm) in CHS, the experimental results with Ti-gettering give a hollow density profile for ECH and a peaked density profile for NBI. Further understanding is needed to explain the formation of the electron density profile. The electron temperature obtained changes a lot for the boronization case. The central electron temperature reaches to 400 eV. This level is close to NBI case of 1 MW injection. Higher electron temperatures are also obtained when an ECH pulse is added during the ICRF plasma.

The electron temperatures are plotted as a function of the electron density in Fig. 4. The electron temperature is obtained from the diamagnetic energy under assumptions of $T_e = T_i$, $Z_{eff} = 3$, and parabolic profile of the

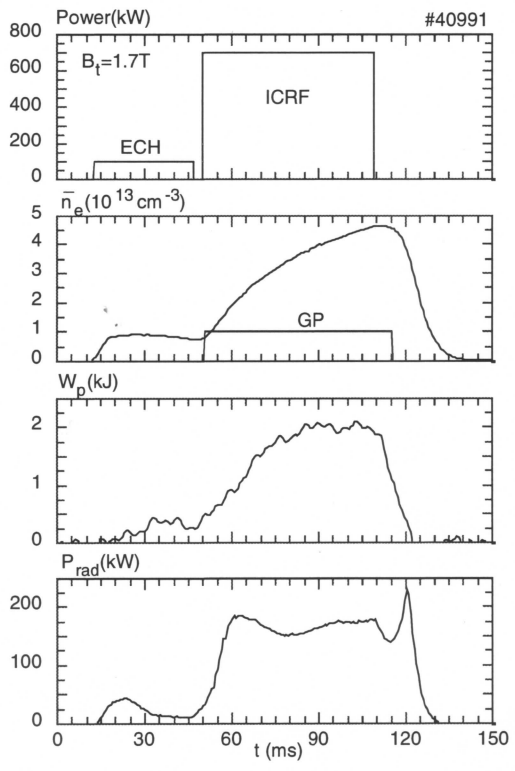

Fig. 2. Time trace for typical ICRF result after boronization.

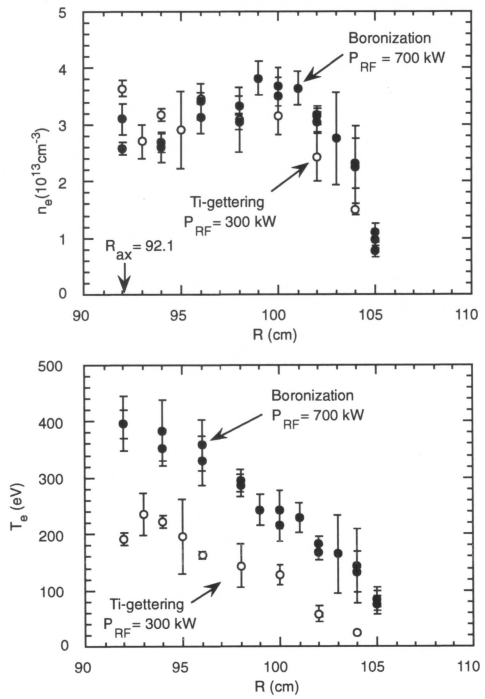

Fig. 3. Comparison of electron density (upper) and electron temperature (lower) profiles.

temperatures. The result obtained for the boronization case shows constant electron temperature below 3×10^{13} cm^{-3} and it slowly decays above the density. Then, the increase in the W_p shown in Fig.1 comes from the increase in the electron density. The density of 3×10^{13}cm^{-3} at which the W_p saturates probably depends on the injected power of the ICRF.

In almost all cases of the boronization, large H/D ratios of 50% were observed, because a large amount of hydrogen is introduced by the boronization. The two-ion hybrid resonance is set near the plasma center, and at present it is thought that the electron heating is effective for these ICRF experiments. The estimation of the deposition profile and deposition power is a next step for the study in connection with the scaling analysis as shown in Fig. 1.

Figure 5 shows the relation between the electron temperature and the total radiation power. The ICRF power injected was 700 kW. The electron temperature does not show any change for P_{rad} more than 250 kW and keeps a constant low temperature. However, the temperature increases rapidly when the P_{rad} decreases below 250 kW. A small change in the P_{rad} gives a large change in the electron temperature. This result indicates that the central electron temperature is related to the local balance of the P_{rad}, especially in an edge region.

Finally, we can estimate impurity concentration for the typical results of the Ti-gettering and boronization cases:

Ti-gettering: P_{rf} = 300 kW, $n_e = 1.8 \times 10^{13}$ cm^{-3}, T_e = 240 eV, P_{rad} = 150 kW, Z_{eff} = 3

Boronization: P_{rf} = 300 kW, n_e=3.2 $\times 10^{13}$ cm^{-3}, T_e=240 eV, P_{rad} = 120 kW, Z_{eff} = 3.

The total radiation consists of 80 kW oxygen, 40 kW titanium, and 30 kW others (hydrogen, carbon, nitrogen) for the Ti-gettering case. For the boronization case, it consists of 25 kW oxygen and others. The main part of the remaining radiation in the boronization case is estimated to be from the boron itself. The guard limiters of the antennas are made of stainless steel (SS). The impurity concentration can be estimated from these results with the observation of the Z_{eff}. For the Ti-gettering shot the impurity concentration was 1% for carbon, 1.5% for oxygen, 0.5% for titanium; and for the boronization shot it was 5% for boron, 1% for carbon, 0.5% for oxygen, and 0% for titanium. However, we have to say at least that computations from the impurity transport code always give us a certain difference between measured Z_{eff} and measured radiation power from each of the impurity ions such as O V. Then, the impurity concentration mentioned above is obtained by a normalization to the measured Z_{eff} values. Further under-

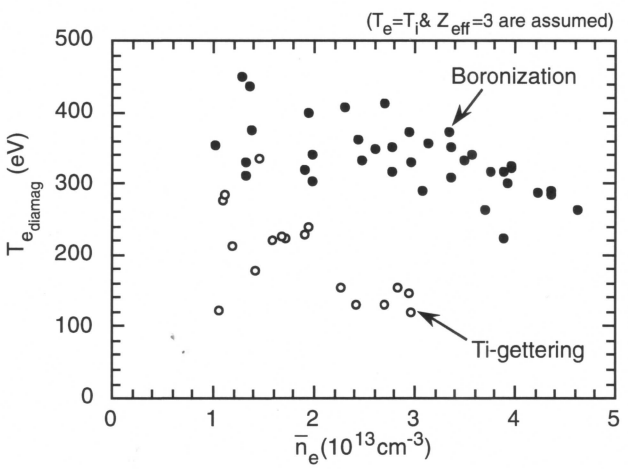

Fig. 4. Electron temperature as a function of line-averaged electron density. The RF power is 700 kW for both cases.

standing for the impurity transport, especially in the edge region, will bring a consistency between the calculation and experiment in such a problem.

Shigeru Morita for CHS Group
National Institute for Fusion Science
Nagoya 464-01, Japan

E-mail: morita@rdsrvr.nifs.ac.jp

Reference

[1] H. Yamada and S. Morita et. al., submitted to Jpn. J. Appl. Phys.

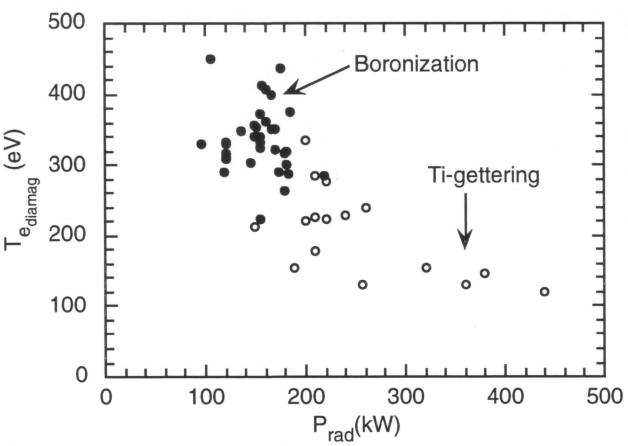

Fig. 5. Electron temperature as a function of total radiation loss. The RF power is 700 kW for both cases.

First results from the new NIR Z_{eff} diagnostic on W7-AS

The effective ion charge Z_{eff} is one of the main parameters for characterizing the purity of a fusion plasma. Increased values of Z_{eff} indicate fuel dilution and possibly enhanced energy loss from the plasma due to additional line and continuum radiation. Neoclassical transport, too, depends on Z_{eff}. Therefore, it is of uppermost importance to have a reliable routine measurement of Z_{eff}.

The flux of bremsstrahlung, emitted from the plasma, depends almost linearly on the value of Z_{eff}. Its emissivity has a maximum, for typical plasma parameters (T_e ~ 1 keV), in the soft X-ray wavelength range, around λ = 1 nm. This wavelength range is, however, usually dominated by recombination radiation and is therefore not suitable. A sufficient condition, for recombination to be negligible, is $\hbar\omega < Z^2 R_y$, where R_y is the Rydberg energy. This condition is satisfied for visible radiation and longer wavelengths. In performing the Z_{eff} measurement in the visible, one still has to ensure that the intensity is measured in a spectral region that is free from strong impurity line radiation. At low electron density, it has proven difficult on the W7-AS stellarator, as well as other machines, to meet this requirement. By accessing the near infrared spectral region, we try to overcome this difficulty.

Spectroscopically resolved measurements on the stellarator W7-AS as well as on the tokamaks ASDEX and ASDEX-Upgrade [1] show a 50-nm-wide wavelength window in the vicinity of λ ~ 1.04 mm, where line radiation is not apparent (Fig. 1). A 10-nm-wide wavelength range within this line-free interval is used to measure bremsstrahlung, using a PIN silicon diode in combination with an interference filter. A time resolution of 10 kHz is achieved. For each plasma discharge, the spectrally resolved measurement of that wavelength vicinity is also recorded. While the spectral measurement is in most cases not sensitive enough to measure bremsstrahlung quantitatively, at least the absence of line radiation can be verified after each discharge.

Since bremsstrahlung is emitted from the whole volume of a plasma discharge, one can measure it only by integrating along a line of sight, enabling only the deduction of a line-averaged value of Z_{eff}. The geometry of W7-AS allows us to choose a horizontal line of sight, which is nearly tangential to the magnetic axis over a considerable part of its total length. A distance of < 5 cm between the line of sight and the plasma center can be achieved over an integration length of about 1.4 m. Therefore, the measurement is heavily weighted

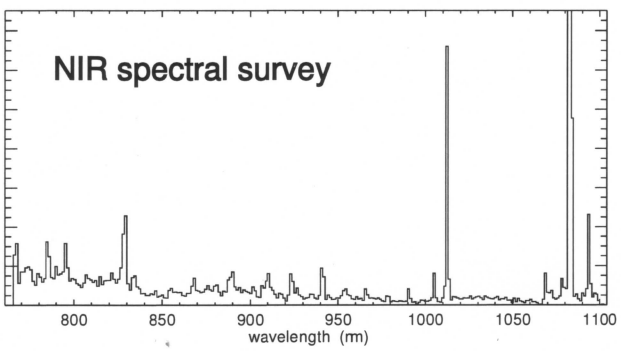

Fig. 1. Survey spectrum of the near infrared spectral region. The spectrum is composed of 16 individual measurements, which have been conducted in subsequent plasma discharges with a 35-element Si-OMA detector.

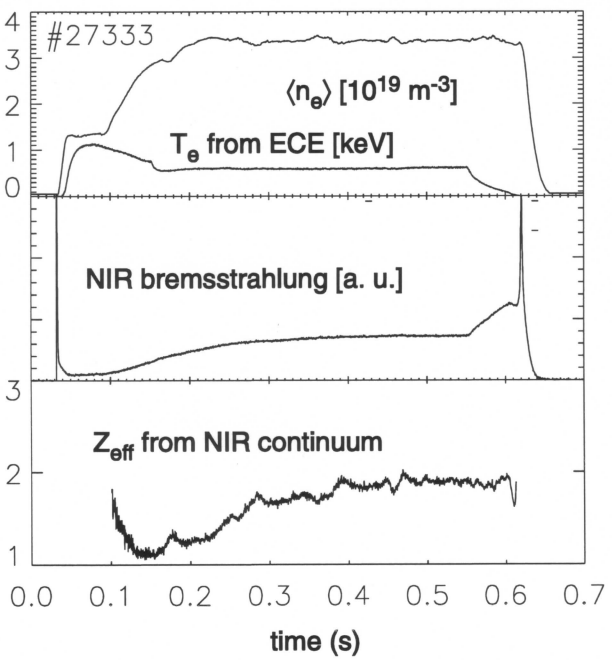

Fig. 2. Time traces of n_e, T_e, and NIR bremsstrahlung during a 200-kW ECRH discharge. Z_{eff}, which is deduced from those three measurements, is shown only where n_e is higher than 1.5 ö 10^{19} m^{-3}.

toward the plasma center, so that we are able to deduce central values of Z_{eff} without recourse to inversion methods.

The new Z_{eff} diagnostic has been operating routinely and reliably on W7-AS since the middle of May. Figure 2 shows the time trace of bremsstrahlung for W7-AS shot 27333. The typical features are the recombination radiation peaks at the beginning and the end of the discharge and the increase of bremsstrahlung during the temperature collapse of the discharge, after ECRH has terminated. The increase of bremsstrahlung at the end of the discharge is fully explained by the decreasing temperature, so that Z_{eff} remains constant after the turn-off time of plasma heating. The noise on the deduced Z_{eff} is predominantly caused by the noise on the n_e measurement. In Fig. 2 the n_e signal has been smoothed with a time constant of 10 ms. A small level of spectrally unresolved background radiation limits the sensitivity of the Z_{eff} measurement to plasmas with n_e above 1.5 ö1 0^{19} m^{-3}.

Since the commencement of the new diagnostic we have been able to follow the evolution of Z_{eff} in many 70/140-GHz ECR and co/counter NBI-heated discharges. For the near future, we envisage studying aspects of possible impurity accumulation during the different heating schemes and at various magnetic field configurations.

W. Mandl
IPP Garching, Germany
Phone : 0049-89-3299-1492

E-Mail: mandl@ipp-garching.mpg.de

References

[1] H.Röhr, K.H.Steuer, Rev.Sci.Inst **59** (1988) 8.